Journal of Inorganic and Organometallic Polymers and Materials (2018) 28:1728–1738
https://doi.org/10.1007/s10904-018-0820-0

Dye Adsorption on Cubic Polyhedral Oligomeric Silsesquioxane-Based Poly(acrylamide-*co*-itaconic acid) Hybrid Nanocomposites: Kinetic, Thermodynamic and Isotherms Studies

Bagher Eftekhari-Sis[1] · Ali Akbari[1] · Parisa Yekan Motlagh[1] · Zahra Bahrami[1] · Nasser Arsalani[2]

Received: 9 January 2018 / Accepted: 1 March 2018 / Published online: 7 March 2018

Abstract
In the present study, poly(acrylamide-*co*-itaconic acid) hybrid nanocomposites were synthesized via free radical copolymerization method. Octavinyl polyhedral oligomeric silsesquioxane (OV-POSS) with different weight ratio (0, 4, 8, 12 and 14 wt%) was utilized as a cross-linker. Dye adsorption properties of the as-prepared hybrid nanocomposites were investigated for crystal violet (CV) elimination from aqueous solution. The effect of various parameters, such as OV-POSS content, adsorbent amount, pH, temperature, contact time and initial dye concentration, on the adsorption of CV was studied. Moreover, adsorption kinetic, isotherm and the thermodynamic of the CV adsorption on the so-called hybrid nanocomposites were studied.

Keywords Dye adsorption · Poly(acrylamide-*co*-itaconic acid) · POSS · Nanocomposites · Crystal violet

1 Introduction

In the past decades, rapid industrialization has led to rise dramatically human and environmental exposure to discharged wastewater containing toxic organic dyes and heavy metals. Among them, remarkable efforts have been devoted to the removal of toxic synthetic dyes due to their high stability and complicated aromatic structures in which caused substantial environmental problems [11, 35]. Crystal violet (CV) as a cationic dye was not only widely used as a purple dye in coloring papers, cottons and wools [17], but also used as an active ingredient in Gram's stain as well as bacteriostatic agent in medical community [23]. Beside these applications, some serious detrimental side effects of CV involving vomiting, cyanosis, heartbeat increase and tissue necrosis in humans were observed [15]. All above mentioned dangerous effects inspired the human community to eradicate the CV from industrial effluents before releasing it into the environment. Various conventional techniques such as physicochemical and biological treatments have been exploited for the elimination of CV from wastewaters [12, 26]. Among them, adsorption could be recognized as a superior technique in comparison with other techniques for dye traces decontamination from wastewater because of its low cost, ease of operation, regeneration possibility of used adsorbent, simplicity of design and lack of secondary pollution [21, 28, 38]. Until now, various materials have been investigated for dye removal, such as activated carbon, polysaccharides, clay, zeolite, hydrogels, and polymeric materials. Out of the mentioned materials, hydrogels and polymeric compounds with various functional groups ($–NH_2$, –OH and –COOH) have gained much more concerns as effective adsorbents [10]. Although polymeric materials have many advantageous in pollutants removal, the low thermal and mechanical strength of these materials could be assumed as the major drawback and limited their practical applications in the adsorption processes. So incorporation of inorganic nano fillers into the polymeric materials structure can be assumed as an efficient strategy for solving the problem [5, 37]. In this way, the exploration and application of new nano fillers is still desirable.

Over the years, design and fabrication of novel organic–inorganic polymeric nanocomposites has been

✉ Bagher Eftekhari-Sis
eftekhari.sis@gmail.com; eftekharisis@maragheh.ac.ir

[1] Department of Chemistry, University of Maragheh, Maragheh 55181-83111, Iran

[2] Polymer Research Laboratory, Department of Organic and Biochemistry, Faculty of Chemistry, University of Tabriz, Tabriz, Iran

the focus of research for materials scientists [18, 20, 27]. Recently, polyhedral oligomeric silsesquioxane (POSS), as a new type of nanostructured hybrid materials, has gained considerable interests in the preparation of hybrid polymeric nanocomposites. POSS nano-bulding has the general formula of $(RSiO_{1.5})_{2n}$. It is often considered as an intermediate between silica (SiO_2) and silicones (R_2SiO) with a symmetrical cage-like three dimensional structure and eight organofunctional groups in outer shell [2, 3, 31]. Compared with other nanoparticles such as metal oxides, silica, layered silicates and carbon nanotubes, the advantageous of POSS nanobuildings lie mainly in their versatile reactivity, nanosized structure from 1 to 3 nm in diameter and well-dispersion in polymeric matrices. POSS units can be introduced to all polymer types either by grafting [14, 30], blending [34] or copolymerization reactions [19, 36]. Due to their simplicity processing and the excellent physicochemical properties, POSS-based materials are becoming the focus of many applications including electronics, tissue engineering, catalysis, energy, mechanics, sensors, medicine and so forth [16]. Among these applications, using POSS-based hybrid polymeric materials as adsorbents for environmental wastewater remediation has gained less attention. For instance, just in one report, Akbari and Arsalani utilized organic–inorganic hybrid of incompletely condensed polyhedral oligomeric silsesquioxane (IC-POSS) nanoparticles and poly (acrylamide-*co*-hydroxyethyl methacrylate) for cleaning wastewaters from methylene blue as toxic dye [1]. In addition, some other adsorbents based on POSS materials have been reported. For example, in recent years, Filho and coworkers directly functionalized the eight arms of completely condensed POSS with organic functional groups, including 2,2-dipyridylamine [32], 2-amino-1,3,4-thiadiazole [29], 3-amino-1,2,4-triazole [6] and thiourea [33], and used for the adsorption of heavy metals from aquatic systems. To the best of our knowledge, there has been no precedent report on the use of completely condensed POSS-based polymeric materials as adsorbent in the elimination of toxic dyes from wastewaters.

In this contribution, for the first time we have designed and synthesized an organic–inorganic adsorbent, including completely condensed silsesquioxane with eight vinyl groups (OV-POSS) and copolymer of acrylamide (AAm) and itaconic acid (IA) monomers by precipitation polymerization, as a new adsorbent for the adsorption of crystal violet (CV). Incorporation of the sole building blocks of OV-POSS in the structure of the poly(AAm-*co*-IA) matrices increased the hydrophobicity of the copolymer and makes them as an ideal candidate in adsorption processes.

2 Experimental

2.1 Materials

Itaconic acid (IA), acrylamide (AAm) and octavinyl polyhedral oligomeric silsesquioxane (OV-POSS) monomers were purchased from Sigma-Aldrich. Azobis(isobutyronitrile) (AIBN), also from Sigma-Aldrich, was recrystallized from methanol before use. Solvents such as tetrahydrofuran (THF), acetone, acetonitrile, and *n*-hexane were obtained from Merck Co. THF was dried on Na/benzophenone under a nitrogen atmosphere immediately before use.

2.2 Instrumentation

Fourier transform infrared (FT-IR) spectra were carried out on a Win-Bomem spectrometer, version 3.04 Galactic Industries Corporation over the range of 400–4000 cm^{-1}. The scanning electron microscopy (SEM) analyses were done by a VWGA3 TESCAN (20.0 KV) microscope field emission scanning electron microscope (FE-SEM) at an accelerating voltage of 20 kV with an energy-dispersive X-ray (EDX) spectroscopy. The XRD diffraction patterns of samples was collected with a Bruker D8 Advance diffractometer using a Cu Kα radiation source ($\lambda = 0.154059$ nm) at 30 keV in the scan range (2θ) from 4° to 70°. Thermogravimetric (TGA) analyses were performed using a Linseis L81A1750 (Germany) at a heating rate of 10 °C/min under high purity nitrogen atmosphere from 50 to 800 °C. UV–Vis absorption spectra were recorded on a Shimadzu UV-1800 model spectrophotometer.

2.3 Preparation of Hybrid Nanocomposites

Hybrid nanocomposites, poly(AAm-*co*-IA)/OV-$POSS_n$, were synthesized by precipitation polymerization of acrylamide with itaconic acid in the presence of various amount of OV-POSS. Typically, 50 mL three-necked round bottom flask containing 10 mL dried THF equipped with a reflux condenser and N_2 inlet was used. First, 0.16 g acrylamide (2.25 mmol), 0.04 g itaconic acid (0.31 mmol), 1 wt% AIBN relative to the monomers and the desired amount of OV-POSS were charged into the flask and purged with nitrogen under stirring for 30 min. Then, the precipitation polymerization was initiated by immersing the flask into a 70 °C water bath. The reaction mixture became milky after 30 min and a sticky white solid was obtained after 3 h. The formed poly(AAm-*co*-IA)/OV-$POSS_n$ hybrid nanocomposites were centrifuged and washed 3 times with each THF and *n*-hexane and dried in vacuum at 50 °C for 48 h to obtain a white powder. In addition, The

poly(AAm-*co*-IA) was synthesized without OV-POSS as control using the same conditions.

2.4 Dye Adsorption

First of all, in order to have the calibration curve to determine the concentrations of CV, a series of diluted CV solutions was subjected to a UV–Vis spectrophotometer at 586 nm. The equation of calibration curve was $A = 0.1779 \times C$ (with high regression coefficient value; $r^2 = 0.9816$) in the range of 0–16 mg/L of CV concentrations, where C (mg/L) is the concentration of CV and A is the absorbance of CV at $\lambda_{max} = 586$ nm. Various parameters, such as OV-POSS content of poly(AAm-*co*-IA)/OV-POSS$_n$, amount of adsorbent, pH, contact time, temperature, CV initial concentrations and salt effects were studied in order to evaluate the adsorption efficiency of hybrid nanocomposites. To study the CV adsorption, desired amount of hybrid nanocomposites, was added into 10 mL of CV solutions with identical concentration (mg/L) at certain pH in flask. After reaching equilibrium, the concentration of CV left in the supernatant solution was measured using UV–Vis spectrophotometer. Equilibrium adsorption, q_e (mg/g), was calculated using Eq. (1).

$$q_e = \frac{(C_0 - C_e)}{W} \times V \quad (1)$$

where C_0 and C_e are the initial and equilibrium concentrations of CV (mg/L), W is the adsorbent weight (g), and V is the volume of the solution (L).

3 Results and Discussion

3.1 Synthesis of Hybrid Polymeric Nanocomposites

Having suitable functional groups, water insolubility and excellent physical properties are substantial for materials to be as an ideal dye adsorbent. In this regard, by embedding different feed ratio of OV-POSS into the copolymer of the AAm and IA, novel series of hybrid polymeric nanocomposites were prepared via precipitation polymerization. The synthesis of hybrid polymeric nanocomposite is outlined in Fig. 1.

It is noteworthy that with the increasing OV-POSS content, the hydrophobicity of the as-prepared hybrid nanocomposites, poly(AAm-*co*-IA)/OV-POSS$_n$, is increased. The solubility of the synthesized nanocomposites in various solvents was investigated, which was summarized in Table 1. Prepared nanocomposites are insoluble in common organic solvent, except DMSO as a more polar solvent. Presence of amide and carboxylic acid functional group led to the solubility of the poly(AAm-*co*-IA) in

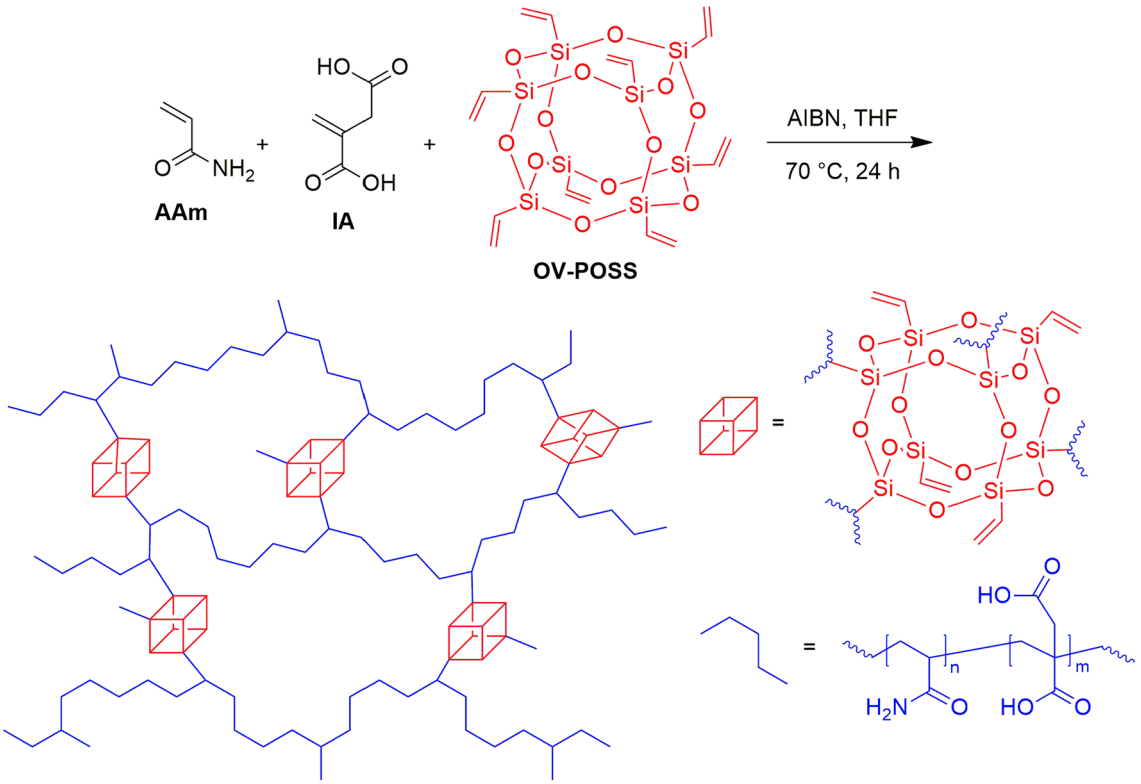

Fig. 1 Preparation of poly(AAm-*co*-IA)/OV-POSS$_n$ hybrid nanocomposites

Table 1 Solubility of the polymeric nancomposites in various solvents

Solvent	Poly(AAm-*co*-IA)	Poly(AAm-*co*-IA)/OV-POSS$_n$ (n)			
		4	8	12	14
CH_2Cl_2	×	×	×	×	×
DMF	×	×	×	×	×
THF	×	×	×	×	×
Toluene	×	×	×	×	×
DMSO	√	√	√	√	√
Water	√	√[a]	×	×	×

√ soluble, × insoluble

[a]Soluble in warm water

water through hydrogen bonding. By increasing the POSS as a cross linker in the nanocomposites structure, the water solubility is decreased.

3.2 Characterization of Hybrid Polymeric Nanocomposites

3.2.1 FT-IR Spectra

To confirm the functional groups and presence of OV-POSS nanoparticles in the structure of the poly(AAm-*co*-IA)/OV-POSS$_n$, FT-IR spectra of pure OV-POSS, poly(AAm-*co*-IA) and poly(AAm-*co*-IA)/OV-POSS$_n$ with n = 4, 8, 12 and 14 wt% are illustrated in Fig. 2. FT-IR spectrum of OV-POSS shows some main characteristic peaks. An important peak at 1122 cm^{-1} is related to the stretching vibration of Si–O groups, which is a clear witness for the existence of silsesquioxane cages [9]. In the case of poly(AAm-*co*-IA), the peaks at 3427 and 3205 cm^{-1} are attributed to N–H and O–H stretching vibrations, respectively. The stretching and bending vibrations of methylene groups are found at 2938 and 1436 cm^{-1}, respectively. Peaks at 1665 cm^{-1} with a shoulder could be related to stretching vibrations of C=O of amide and carboxylic acid functional groups. Bands at 1330 and 1204 cm^{-1} are accounting to vibrations of C–N and C–O bonds, respectively. The spectra of all poly(AAm-*co*-IA)/OV-POSS$_n$ hybrid nanocomposites are similar to that of poly(AAm-*co*-IA) except that a strong peak appears at 1121 cm^{-1}, which proves successful incorporation of OV-POSS cage into the polymeric matrices. Moreover, the intensity of this band increases with the increase of the OV-POSS feed ratio, which can be assumed as another clear evidence for the incorporation of OV-POSS into the hybrid nanocomposites [2].

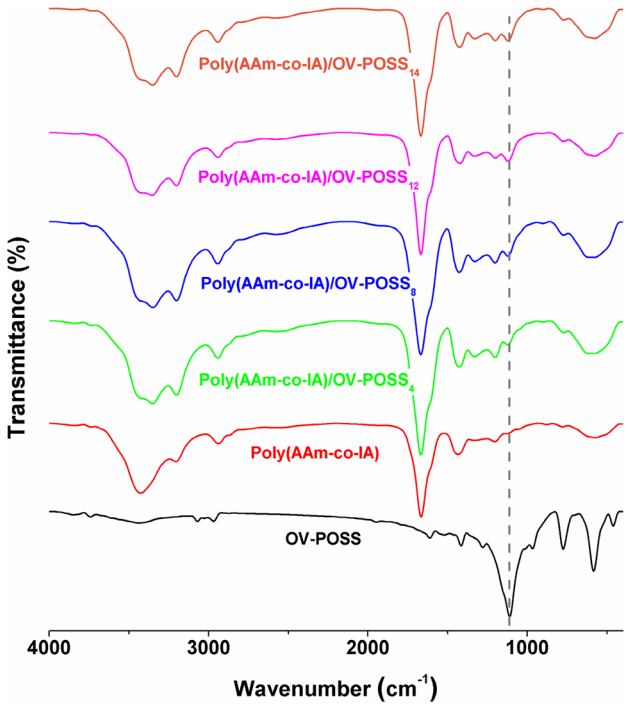

Fig. 2 FT-IR spectra of OV-POSS, poly(AAm-*co*-IA) and poly(AAm-*co*-IA)/OV-POSS$_n$ (n = 4, 8, 12 and 14)

3.2.2 NMR Spectra

In order to confirm the incorporation of OV-POSS into the structure of hybrid nanocomposites, ^{1}H NMR spectrum of poly(AAm-*co*-IA)/OV-POSS$_8$ in DMSO-d_6 was recorded. As shown in Fig. 3, protons of CO_2H groups of IA and NH_2 of acrylamide moieties are appeared at 12.11 and 6.85–7.23 ppm, respectively. The ratio of IA/AAm is determined to be 1/7.1, which is in good agreement with used ratio (1/7.2). All protons of aliphatic moieties are shown at 1.31–1.77 and 2.10 ppm, which are assigned in the Fig. 3. Peak at 5.52 ppm is attributed to the unreacted vinyl moieties of OV-POSS, confirming the incorporation of OV-POSS in the polymer as cross linker through a number of its vinyl groups.

3.2.3 XRD Analysis

XRD diffraction patterns of OV-POSS, poly(AAm-*co*-IA) and poly(AAm-*co*-IA)/OV-POSS$_n$ (n = 4, 8 and 12 wt%) are depicted in Fig. 4. The XRD patterns of all poly(AAm-*co*-IA)/OV-POSS$_n$ hybrid nanocomposites are the same as poly(AAm-*co*-IA), exhibiting a broad amorphous diffraction peak at around 2θ = 21.2° related to the polymeric matrix of the poly(AAm-*co*-IA). The disappearance of crystalline peaks of OV-POSS at 2θ = 9.8°, 23.1°

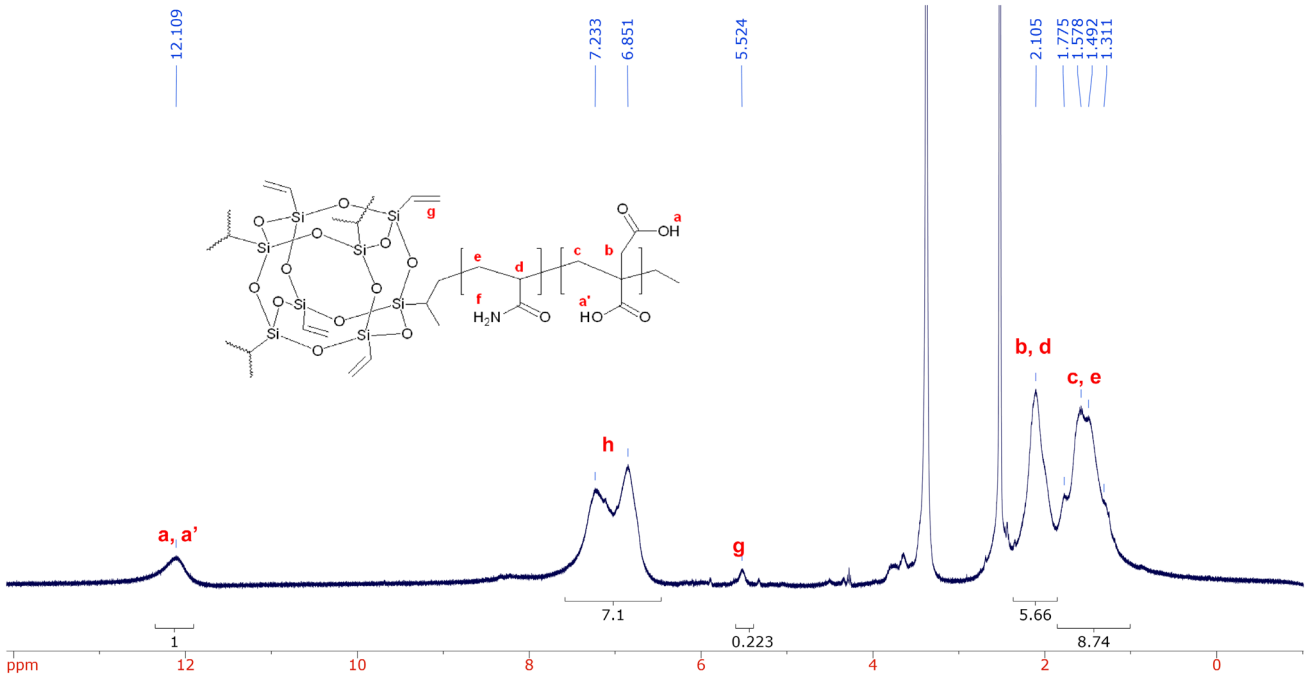

Fig. 3 ^{1}H NMR spectrum of poly(AAm-*co*-IA)/OV-POSS$_8$ in DMSO-d_6 at 400 MHz

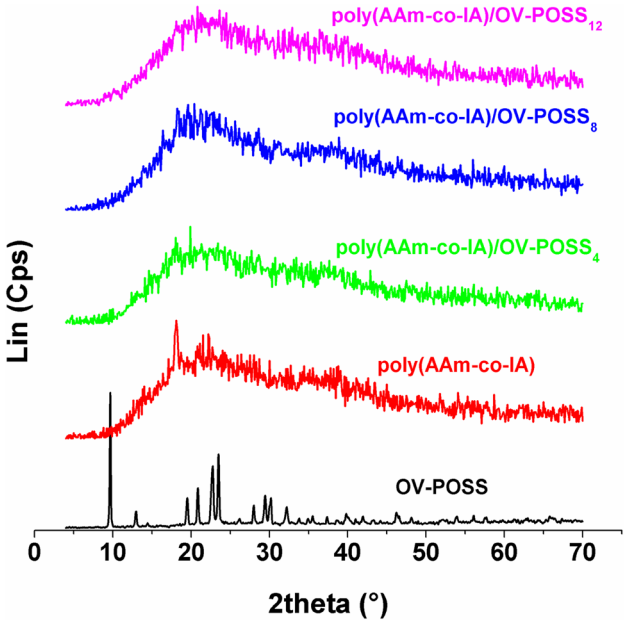

Fig. 4 XRD patterns of OV-POSS, poly(AAm-*co*-IA) and poly(AAm-*co*-IA)/OV-POSS$_n$ (n = 4, 8 and 12)

and 23.9° in the XRD profiles of all poly(AAm-*co*-IA)/OV-POSS$_n$ hybrid nanocomposites confirmed the uniform dispersion of OV-POSS in the structure of organic–inorganic nanocomposites [24].

3.2.4 Morphologies of Hybrid Nanocomposites

SEM images of poly(AAm-*co*-IA) and poly(AAm-*co*-IA)/OV-POSS$_n$ (n = 4 and 8) are illustrated in Fig. 5. According to these images, all materials have similar morphology (spherical particles and uniform size distribution) which are common for polymers fabricated by precipitation method. It is worth to highlight that POSS nanoparticles have very small sizes (1–3 nm), so they could not be directly seen in SEM images [7]. The elemental analyses of poly(AAm-*co*-IA) and poly(AAm-*co*-IA)/OV-POSS$_n$ nanocomposites was investigated by energy dispersive X-ray (EDX) analyses. EDX data of poly(AAm-*co*-IA) showed the existence of C, 68.80%; N, 17.42%; and O, 13.78% elements. In the EDX data of poly(AAm-*co*-IA)/OV-POSS$_n$, in addition to C, N and O elements, Si element was also appeared, in which the W% of Si was increased by increasing the feed ratio of OV-POSS.

3.2.5 Thermal Properties

The thermal stability of poly(AAm-*co*-IA) and poly(AAm-*co*-IA)/OV-POSS$_n$ nanocomposites was studied by TGA analyses. As shown in Fig. 6, poly(AAm-*co*-IA) shows four steps weight loss at 50–90 °C (5.42%) and 150–180 °C (4.94%) for removal of physically adsorbed water molecules, 200–300 °C (13.92%) for decomposition of the side chains and oligomers, and 340–440 °C (47.73%) attributing to the carbonation process of the main chain of

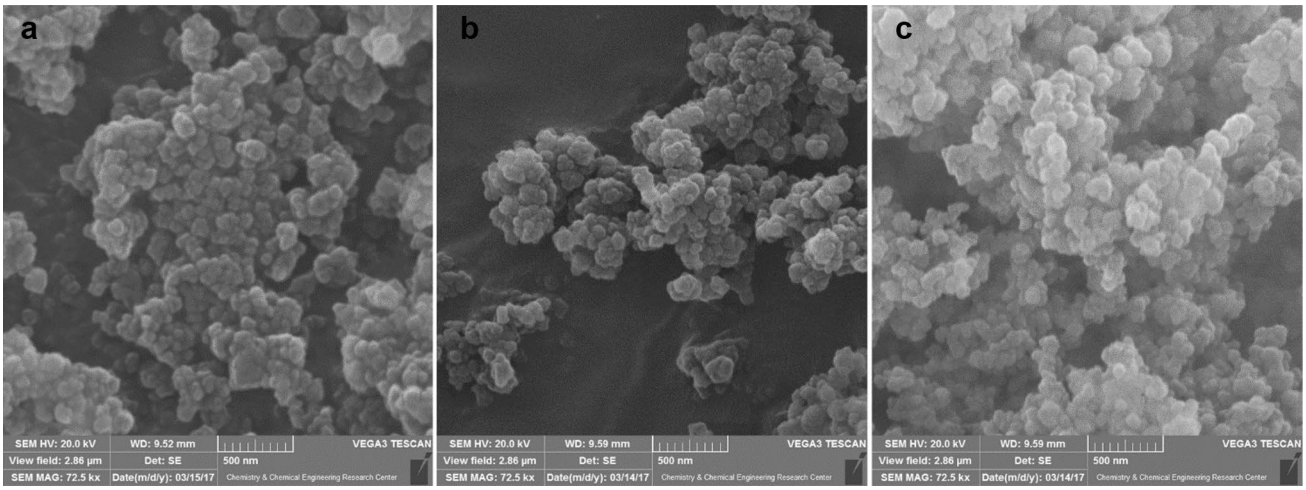

Fig. 5 SEM images of **a** poly(AAm-*co*-IA) and **b** poly(AAm-*co*-IA)/OV-POSS$_4$ and **c** poly(AAm-*co*-IA)/OV-POSS$_8$

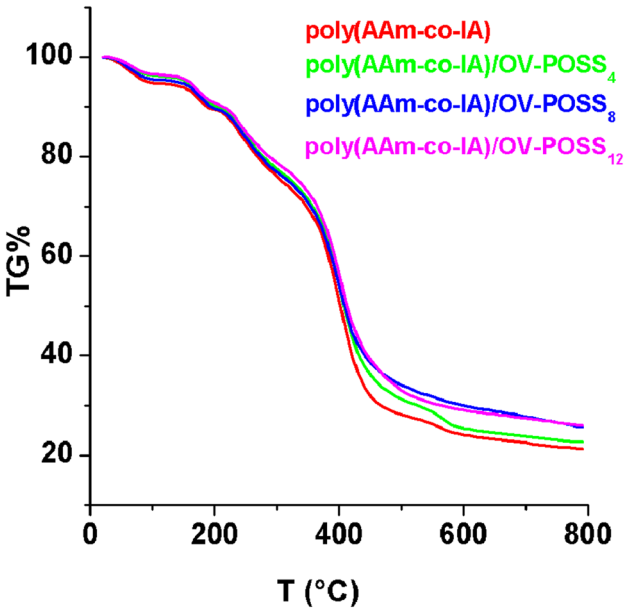

Fig. 6 TGA of poly(AAm-*co*-IA) and poly(AAm-*co*-IA)/OV-POSS$_n$ (n = 4, 8 and 12)

poly(AAm-*co*-IA). The incorporation of POSS as a cross linker in the structure of the poly(AAm-*co*-IA)/OV-POSS$_n$ nanocomposites afforded the higher thermal stability. On the other hand, the fourth weight loss occurred at higher temperature (350–460 °C) and the weight loss was lower than poly(AAm-*co*-IA).

3.3 Dye Adsorption Studies

As all the hybrid nanocomposites, poly(AAm-*co*-IA)/OV-POSS$_n$, have hydrophobicity and abundant carboxylic and amine groups, we assume that they can be utilized as high-performance nanocomposite adsorbents to eliminate pollutants from aqueous media. Herein, crystal violet (CV) as a typical cationic dye was selected for the adsorption studies. Equilibrium adsorption (q_e, mg/g) was calculated according to Eq. (1), and utilized to indicate dye removal efficiency.

3.3.1 The Effect of the Cross Linker

The effect of the cross linker (OV-POSS) content on the adsorption efficiency was studied by addition of 15 mg of adsorbent with different OV-POSS content (4, 8, 12 and 14%) to a solution of CV (5 mL, 100 mg/L) and stirred for 24 h. Nanocomposite with 4 wt% OV-POSS content is solved in water over the time, and therefore shows low equilibrium adsorption. The adsorption efficiency was increased, when the OV-POSS content was reached to 8 wt%. By increasing the content of OV-POSS to 12 and 14 wt%, the dye adsorption capacity of the prepared adsorbents was decreased because of high cross-linking degree of polymeric nanocomposites (Fig. 7a). Therefore, the effect of various parameters including dose of adsorbent, pH, ionic strength, contact time, temperature and CV initial concentrations on the adsorption of CV was investigated on poly(AAm-*co*-IA)/OV-POSS$_8$.

3.3.2 The Effect of pH

The effect of pH on the adsorption of CV was investigated by stirring 5 mL mixture of CV (100 mg/L) and 15 mg of poly(AAm-*co*-IA)/OV-POSS$_8$ at various pH values, and equilibrium adsorption (q_e) was plotted against the pH. Increasing the pH resulted in increasing the q_e value. Increase at pH 3–7 could be related to the deprotonation of carboxylic acid groups and therefore the expansion of

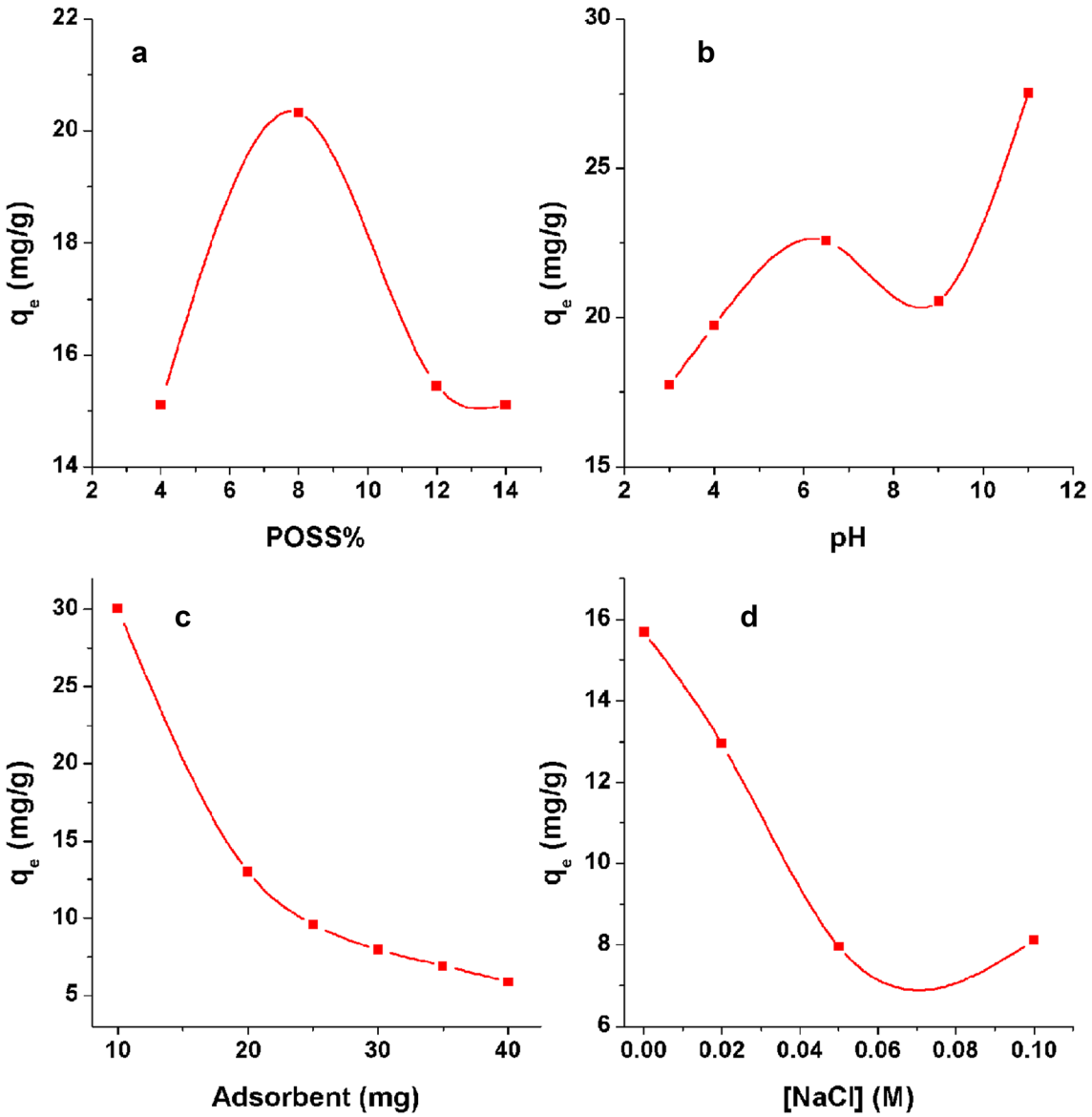

Fig. 7 Effect of **a** OV-POSS content, **b** pH, **c** adsorbent amount and **d** ionic strength on the equilibrium adsorption of CV

the space between polymeric network. Second increase at pH 9–11 is attributed to the strong electrostatic interaction between carboxylate anions and cationic CV molecules (Fig. 7b).

3.3.3 The Effect of the Adsorbent Amount

In order to investigate the effect of amount of the adsorbent, various amount of poly(AAm-*co*-IA)/OV-$POSS_8$ (10–40 mg) was added to 5 mL solution of CV (100 mg/L) at pH 11, and stirred at room temperature for 24 h. As it can be seen from Fig. 7c, by increasing amount of the adsorbent, CV equilibrium adsorption was decreased, which could be attributed to aggregation of nanoparticles in higher dosage. 10 mg of poly(AAm-*co*-IA)/$POSS_8$ exhibited high equilibrium adsorption (q_e), and was selected for further studies.

3.3.4 The Effect of Ionic Strength

The effect of ionic strength on the CV adsorption was investigated by addition of 10 mg of poly(AAm-*co*-IA)/OV-$POSS_8$ to 5 mL of 100 mg/L solutions of CV in the presence of various concentrations of NaCl (0.0–0.1 M) at neutral pH and were stirred at room temperature for 24 h. Due to the competition between Na^+ cations and CV as a cationic dye to adsorb with anionic carboxylate centers, as well as the shielding effect of Na^+ on carboxylate anions, which inhibit the reaching CV to carboxylate centers, equilibrium adsorption (q_e) was decreased

by increasing the concentration of NaCl and accordingly the ionic strength of the solution (Fig. 7d) [13, 22].

3.3.5 Kinetic Models of the Adsorption

By optimum conditions (8 wt% of OV-POSS, pH 11 and 10 mg of adsorbent) in hand, kinetic models of the adsorption was investigated by studying the effect of the contact time on the CV adsorption. Two kinetic models, pseudo-first-order (PFO) and pseudo-second-order (PSO) models were applied to study the adsorption kinetic, by measuring adsorbed CV at different time until equilibrium reached. The nonlinear expression of PFO and PSO kinetic models are as Eqs. (2) and (3), respectively.

$$q_t = q_e\left(1 - e^{-k_1 t}\right) \tag{2}$$

$$q_t = \frac{k_2 q_e^2 t}{1 + q_e k_2 t} \tag{3}$$

where qe and qt (mg/g) are the amount of CV adsorbed on poly(AAm-*co*-IA)/$POSS_8$, at equilibrium condition and time t (min), respectively, and k_1 (1/min) and k_2 (g/mg min) refer to the rate constants of PFO and PSO kinetic models, respectively. Kinetic parameters of PFO and PSO models were calculated by fitting the experimental q_t in the above Eqs. as $q_e = 24.697$ (mg/g) and $k_1 = 1.693$ (1/min) with $r^2 = 0.9828$ and $q_e = 24.909$ (mg/g) and $k_2 = 0.358$ (g/mg·min) with $r^2 = 0.9843$, respectively. As the r^2 values for PFO and PSO models are approximately equal, both PFO and PSO kinetic models were fitted to the experimental data (Fig. 8).

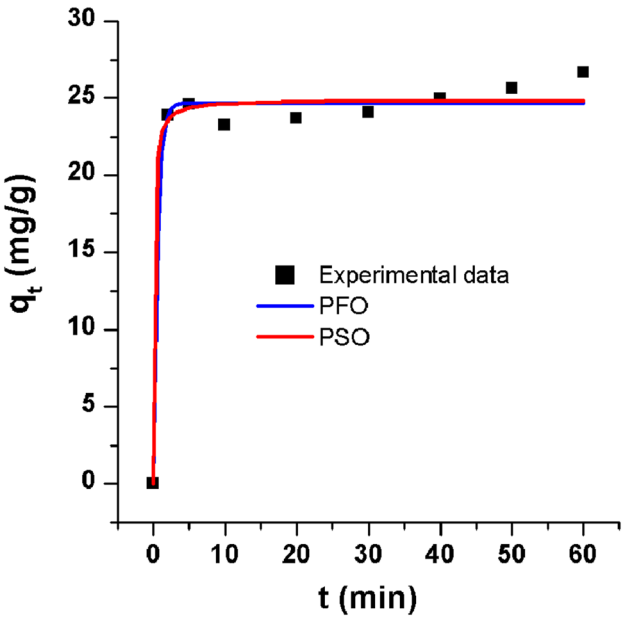

Fig. 8 Adsorption kinetic of CV on poly(AAm-*co*-IA)/$POSS_8$ according to calculated PFO and PSO models

3.3.6 Thermodynamic of the Adsorption

The effect of the temperature on the adsorption of CV on poly(AAm-*co*-IA)/OV-$POSS_8$ was studied, in which by increasing the temperature, q_e was increased and reached to 36.3 mg/g at 60 °C (Fig. 9a). Thermodynamic parameters, including enthalpy change (ΔH, kJ/mol), entropy change (ΔS, kJ/Kmol) and Gibbs free energy (ΔG, kJ/mol) of the adsorption of CV on poly(AAm-*co*-IA)/OV-$POSS_8$, were calculated to predict the mechanism of the absorption, using Eqs. (4)–(7).

$$K_c = \frac{C_s}{C_e} \tag{4}$$

$$\Delta G = -RTLnK_c \tag{5}$$

$$LnK_c = \frac{\Delta S}{R} - \frac{\Delta H}{RT} \tag{6}$$

$$\Delta G = \Delta H - T\Delta S \tag{7}$$

where K_c is the equilibrium constant, C_s and C_e refer to the concentrations of CV adsorbed on poly(AAm-*co*-IA)/OV-$POSS_8$ and in solution at equilibrium condition, respectively. T is absolute temperature in Kelvin (K), and R is the universal gas constant (8.314 Jmol/K). According to Eq. (6), by plotting LnK_c versus 1/T, ΔH and ΔS values were calculated from the slope and intercept of the plot (Fig. 9b), and were found to be 12.086 kJ/mol and 44.319 J/Kmol, respectively. Using Eq. (7), ΔG values were calculated as −1.349, −1.792 and −2.679 kJ/mol at 303, 313 and 333 K, respectively, which are in good agreement with calculated ones using Eq. (5), to be −1.382, −1.741 and −2.698 kJ/mol at 303, 313 and 333 K, respectively. The feasibility and spontaneity of the CV adsorption on poly(AAm-*co*-IA)/$POSS_8$ was concluded by negative values of ΔG. Also, the positive values of ΔH and ΔS support the endothermic process and increase of randomness during the adsorption of CV, respectively.

3.3.7 The Effect of CV Initial Concentration and Adsorption Isotherms

In order to peruse the type of interaction between the poly(AAm-*co*-IA)/OV-$POSS_8$ adsorbent and CV molecules, the effect of initial CV concentration on the equilibrium adsorption was investigated (Fig. 10a). in this regard, two well-known isotherm models (Langmuir and Freundlich isotherm models) [4, 8, 25] were applied to analyze the experimental equilibrium adsorption data (q_e) against the equilibrium concentration of CV. Langmuir and Freundlich models are

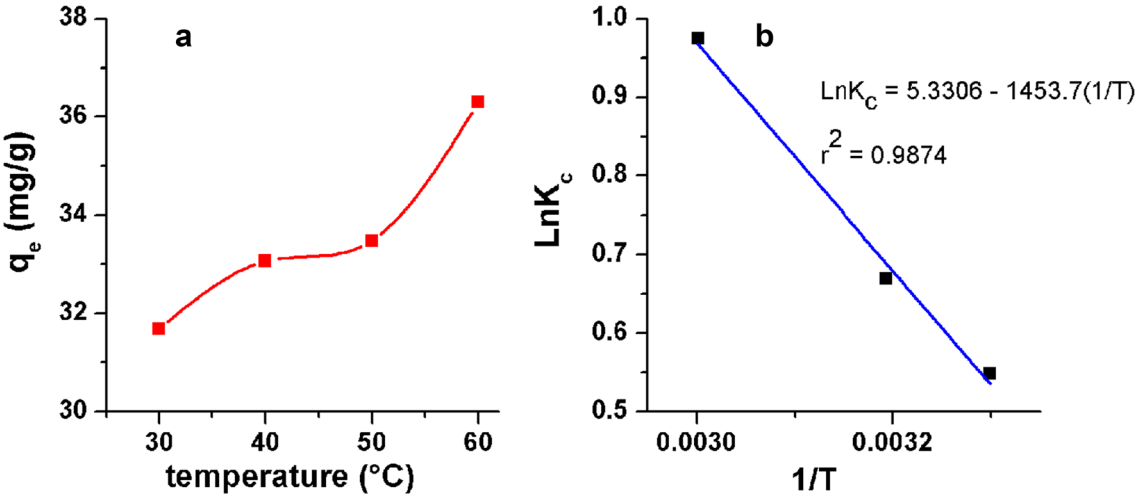

Fig. 9 **a** Effect of temperature on the equilibrium adsorption of CV on poly(AAm-*co*-IA)/$POSS_8$, and **b** plot of LnK_c against 1/T

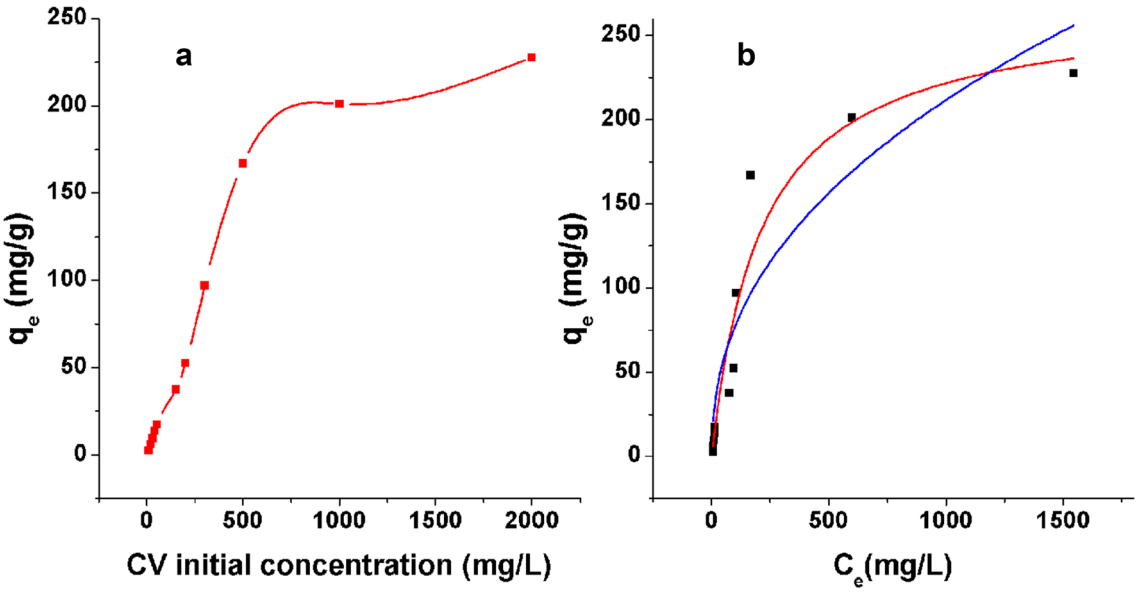

Fig. 10 **a** Effect of the initial concentration of CV on the equilibrium adsorption, and **b** the adsorption isotherm and fitted plots according to Langmuir and Freundlich models of adsorption of CV on poly(AAm-*co*-IA)/$POSS_8$

attributed to a monolayer and uniform adsorption of dye, and a multilayer adsorption of dye on the surface of adsorbent, respectively. The nonlinear expression of Langmuir and Freundlich isotherms are expressed according to Eqs. (8) and (9), respectively.

$$q_e = \frac{q_L K_L C_e}{1 + K_L C_e} \tag{8}$$

$$q_e = K_F C_e^{\frac{1}{n_F}} \tag{9}$$

where q_e (mg/g) is the equilibrium adsorption and C_e (mg/L) is the CV concentration in solution after adsorption at equilibrium condition. q_L (mg/g) and K_L (L/mg) refer to the maximum adsorption capacity and Langmuir constant, the affinity of CV for binding centers of poly(AAm-*co*-IA)/OV-$POSS_8$ adsorbent, respectively. K_F ((mg/g)(L/mg)$^{1/nF}$) and $1/n_F$ are Freundlich constant and heterogeneity factor, respectively. Equilibrium parameter (R_L), from Eq. (10), indicates that Langmuir isotherm is favorable ($0 < R_L < 1$), linear ($R_L = 1$), unfavorable ($R_L > 1$), or irreversible ($R_L = 0$).

$$R_L = \frac{1}{1 + K_L C_0} \tag{10}$$

where C_0 is the highest initial CV concentration.

Figure 10b shows the fitted plots according to Langmuir and Freundlich models for the adsorption of CV on poly(AAm-*co*-IA)/OV-POSS$_8$ adsorbent and the constant parameters (q_e = 268.80 mg/g and k_L = 0.00472 L/mg with r^2 = 0.9287 for Langmuir isotherm, and k_F = 10.35 (mg/g)(L/mg)$^{1/nF}$ and n_F = 2.2884, with r^2 = 0.8412 for Freundlich isotherm) were obtained based on the experimental data. r^2 is correlation coefficient, and the high r^2 value for Langmuir model, revealed that the adsorption occurred homogenously through a monolayer adsorption on the surface of adsorbent. Also, the value of R_L = 0.096, revealed the favorable Langmuir isotherm.

4 Conclusion

In conclusion, a new series of polymeric hybrid nanocomposites based on poly(AAm-*co*-IA) possessing octavinyl polyhedral oligomeric silsesquioxane (OV-POSS) as a cross linker was synthesized via precipitation copolymerization. The solubility of the polymeric hybrid nanocomposites was controlled by the feed ratio of OV-POSS. Synthesized nanocomposites were examined for crystal violet (CV) removal from aqueous solutions. Polymeric nanocomposite with 8 wt% OV-POSS content shows a high adsorption capacity toward CV. Pseudo-first-order and pseudo-second-order kinetic models were applied to investigate the kinetic of the adsorption. The thermodynamic of the adsorption was also studied, by measuring equilibrium adsorption at different temperatures. Moreover, the adsorption isotherm of the CV adsorption on polymeric hybrid nanocomposite, poly(AAm-*co*-IA)/OV-POSS$_{8,}$ was studied using Langmuir and Freundlich isotherm models. Simple preparation of nanocomposite using nontoxic POSS cross linker, and high equilibrium adsorption (230 mg/g) at high concentrations of CV are some advantages of this protocol.

Acknowledgements We are grateful to the University of Maragheh for financial support. Corresponding author thanks the Iran Science Elites Federation (ISEF).

References

1. A. Akbari, N. Arsalani, Organic–inorganic incompletely condensed polyhedral oligomeric silsesquioxane-based nanohybrid: synthesis, characterization and dye removal properties. Polym. Plast. Technol. Eng. **55**(15), 1586–1594 (2016)
2. A. Akbari, N. Arsalani, Preparation and characterization of novel hybrid nanocomposites by free radical copolymerization of vinyl pyrrolidone with incompletely condensed polyhedral oligomeric silsesquioxane. J. Inorg. Organomet. Polym Mater. **26**(3), 536–544 (2016)
3. A. Akbari, N. Arsalani, M. Amini, E. Jabbari, Cube-octameric silsesquioxane-mediated cargo copper Schiff base for efficient click reaction in aqueous media. J. Mol. Catal. A **414**, 47–54 (2016)
4. M. Belhachemi, F. Addoun, Comparative adsorption isotherms and modeling of methylene blue onto activated carbons. Appl. Water Sci. **1**(3–4), 111–117 (2011)
5. D. Cangialosi, A. Alegría, J. Colmenero, Effect of nanostructure on the thermal glass transition and physical aging in polymer materials. Prog. Polym. Sci. **54**, 128–147 (2016)
6. N.L. Dias Filho, F. Marangoni, R.M. Costa, Preparation, characterization, and CuX_2 and CoX_2 (X = Cl–, Br–, ClO_4–) adsorption behavior of a polyhedral oligomer silsesquioxane functionalized with an organic base. J. Colloid Interface Sci. **313**(1), 34–40 (2007)
7. J. Duan, E. Litwiller, I. Pinnau, Preparation and water desalination properties of POSS-polyamide nanocomposite reverse osmosis membranes. J. Membr. Sci. **473**, 157–164 (2015)
8. K. Foo, B. Hameed, Insights into the modeling of adsorption isotherm systems. Chem. Eng. J. **156**(1), 2–10 (2010)
9. J. Fu, L. Shi, Y. Chen, S. Yuan, J. Wu, X. Liang, Q. Zhong, Epoxy nanocomposites containing mercaptopropyl polyhedral oligomeric silsesquioxane: morphology, thermal properties, and toughening mechanism. J. Appl. Polym. Sci. **109**(1), 340–349 (2008)
10. S. Ghorai, A. Sarkar, M. Raoufi, A.B. Panda, H. Schönherr, S. Pal, Enhanced removal of methylene blue and methyl violet dyes from aqueous solution using a nanocomposite of hydrolyzed polyacrylamide grafted xanthan gum and incorporated nanosilica. ACS Appl. Mater. Interfaces **6**(7), 4766–4777 (2014)
11. V. Gupta, Application of low-cost adsorbents for dye removal–a review. J. Environ. Manage. **90**(8), 2313–2342 (2009)
12. F.I. Hai, K. Yamamoto, K. Fukushi, Hybrid treatment systems for dye wastewater. Crit. Rev. Environ. Sci. Technol. **37**(4), 315–377 (2007)
13. Y. Hu, T. Guo, X. Ye, Q. Li, M. Guo, H. Liu, Z. Wu, Dye adsorption by resins: effect of ionic strength on hydrophobic and electrostatic interactions. Chem. Eng. J. **228**, 392–397 (2013)
14. D. Jiang, L. Liu, J. Long, L. Xing, Y. Huang, Z. Wu, X. Yan, Z. Guo, Reinforced unsaturated polyester composites by chemically grafting amino-POSS onto carbon fibers with active double spiral structural spiralphosphodicholor. Compos. Sci. Technol. **100**, 158–165 (2014)
15. A. Kunz, H. Mansilla, N. Duran, A degradation and toxicity study of three textile reactive dyes by ozone. Environ. Technol. **23**(8), 911–918 (2002)
16. S.-W. Kuo, F.-C. Chang, POSS related polymer nanocomposites. Prog. Polym. Sci. **36**(12), 1649–1696 (2011)
17. S. Li, Removal of crystal violet from aqueous solution by sorption into semi-interpenetrated networks hydrogels constituted of poly (acrylic acid-acrylamide-methacrylate) and amylose. Bioresour. Technol. **101**(7), 2197–2202 (2010)
18. K.K. Maniar, Polymeric nanocomposites: a review. Polym. Plast. Technol. Eng. **43**(2), 427–443 (2004)
19. Y. Mao, Q. Zhao, J. Wu, T. Pan, B. Zhou, Y. Tian, A highly sensitive and fast-responding oxygen sensor based on POSS-containing hybrid copolymer films. J. Mater. Chem. C **5**(44), 11395–11402 (2017). https://doi.org/10.1039/C7TC03606J
20. J.E. Mark, Some novel polymeric nanocomposites. Acc. Chem. Res. **39**(12), 881–888 (2006)
21. F. Marrakchi, W. Khanday, M. Asif, B. Hameed, Cross-linked chitosan/sepiolite composite for the adsorption of methylene blue and reactive orange 16. Int. J. Biol. Macromol. **93**, 1231–1239 (2016)
22. N.S. Maurya, A.K. Mittal, P. Cornel, E. Rother, Biosorption of dyes using dead macro fungi: effect of dye structure, ionic strength and pH. Bioresour. Technol. **97**, 512–521 (2006)

23. A. Mittal, J. Mittal, A. Malviya, D. Kaur, V. Gupta, Adsorption of hazardous dye crystal violet from wastewater by waste materials. J. Colloid Interface Sci. **343**(2), 463–473 (2010)
24. O. Monticelli, A. Fina, A. Ullah, P. Waghmare, Preparation, characterization, and properties of novel PSMA—POSS systems by reactive blending. Macromolecules **42**(17), 6614–6623 (2009)
25. H. Qiu, L. Lv, B.C. Pan, Q.J. Zhang, W.M. Zhang, Q.X. Zhang, Critical review in adsorption kinetic models. J. Zhejiang Univ. Sci. A **10**(5), 716–724 (2009)
26. H.S. Rai, M.S. Bhattacharyya, J. Singh, T. Bansal, P. Vats, U. Banerjee, Removal of dyes from the effluent of textile and dyestuff manufacturing industry: a review of emerging techniques with reference to biological treatment. Crit. Rev. Environ. Sci. Technol. **35**(3), 219–238 (2005)
27. N. Sabbagh, A. Akbari, N. Arsalani, B. Eftekhari-Sis, H. Hamishekar, Halloysite-based hybrid bionanocomposite hydrogels as potential drug delivery systems. Appl. Clay Sci. **148**(Supplement C), 48–55 (2017). https://doi.org/10.1016/j.clay.2017.08.009
28. S. Sheshmani, A. Ashori, S. Hasanzadeh, Removal of acid orange 7 from aqueous solution using magnetic graphene/chitosan: a promising nano-adsorbent. Int. J. Biol. Macromol. **68**, 218–224 (2014)
29. I.V. Soares, E.G. Vieira, L. Newton Filho, A.C. Bastos, N.C. da Silva, E.F. Garcia, L.J.A. Lima, Adsorption of heavy metal ions and epoxidation catalysis using a new polyhedral oligomeric silsesquioxane. Chem. Eng. J. **218**, 405–414 (2013)
30. B. Song, L. Meng, Y. Huang, Improvement of interfacial property between PBO fibers and epoxy resin by surface grafting of polyhedral oligomeric silsesquioxanes (POSS). Appl. Surf. Sci. **258**(24), 10154–10159 (2012)
31. K. Tanaka, Y. Chujo, Advanced functional materials based on polyhedral oligomeric silsesquioxane (POSS). J. Mater. Chem. **22**(5), 1733–1746 (2012)
32. E.G. Vieira, I.V. Soares, N.L. Dias Filho, N.C. da Silva, S.D. Perujo, A.C. Bastos, E.F. Garcia, T.T. Ferreira, L.F. Fraceto, A.H. Rosa, Study on soluble heavy metals with preconcentration by using a new modified oligosilsesquioxane sorbent. J. Hazard. Mater. **237**, 215–222 (2012)
33. E.G. Vieira, I.V. Soares, G. Pires, R.A. Ramos, D.R. do Carmo, N.L. Dias Filho, Study on determination and removal of metallic ions from aqueous and alcoholic solutions using a new POSS adsorbent. Chem. Eng. J. **264**, 77–88 (2015)
34. H. Xu, S. Tang, J. Chen, N. Chen, Crystalline, thermal, and biodegradable properties of poly (L-lactic acid)/poly (D-lactic acid)/POSS melt blends. Poly. Plast. Technol. Eng. **55**(10), 1000–1011 (2016)
35. M.T. Yagub, T.K. Sen, S. Afroze, H.M. Ang, Dye and its removal from aqueous solution by adsorption: a review. Adv. Colloid Interface Sci. **209**, 172–184 (2014)
36. Z. Zhang, Y. Xue, P. Zhang, A.H. Müller, W. Zhang, Hollow polymeric capsules from POSS-based block copolymer for photodynamic therapy. Macromolecules **49**(22), 8440–8448 (2016)
37. K. Zhou, Q. Zhang, B. Wang, J. Liu, P. Wen, Z. Gui, Y. Hu, The integrated utilization of typical clays in removal of organic dyes and polymer nanocomposites. J. Cleaner Prod. **81**, 281–289 (2014)
38. M. Zirak, A. Abdollahiyan, B. Eftekhari-Sis, M. Saraei, Carboxymethyl cellulose coated Fe_3O_4@ SiO_2 core–shell magnetic nanoparticles for methylene blue removal: equilibrium, kinetic, and thermodynamic studies. Cellulose **25**, 503–515 (2018)